

Article

Superior Strength of Austenitic Steel Produced by Combined Processing, including Equal-Channel Angular Pressing and Rolling

Marina V. Karavaeva *, Marina M. Abramova, Nariman A. Enikeev, Georgy I. Raab and Ruslan Z. Valiev

Institute of Physics of Advanced Materials, Ufa State Aviation Technical University, 12 K. Marx str., Ufa 450008, Russia; abramovamm@yandex.ru (M.M.A.); nariman.enikeev@ugatu.su (N.A.E.); giraab@mail.ru (G.I.R.); rzvaliev@yahoo.com (R.Z.V.)

* Correspondence: karma11@mail.ru; Tel.: +7-917-781-7784

Academic Editor: Hugo F. Lopez

Received: 27 October 2016; Accepted: 29 November 2016; Published: 8 December 2016

Abstract: Enhancement in the strength of austenitic steels with a small content of carbon can be achieved by a limited number of methods, among which is ultrafine-grained (UFG) structure formation. This method is especially efficient with the use of severe plastic deformation (SPD) processing, which significantly increases the contribution of grain-boundary strengthening, and also involves a combination of the other strengthening factors (work hardening, twins, etc.). In this paper, we demonstrate that the use of SPD processing combined with conventional methods of deformation treatment of metals, such as rolling, may lead to additional strengthening of UFG steel. In the presented paper we analyze the microstructure and mechanical properties of the Cr–Ni stainless austenitic steel after a combined deformation. We report on substantial increases in the strength properties of this steel, resulting from a consecutive application of SPD processing via equal-channel angular pressing and rolling at a temperature of 400 °C. This combined loading yields a strength more than 1.5 times higher than those produced by either of these two techniques used separately.

Keywords: stainless steel; severe plastic deformation; strength; ultrafine-grained materials

1. Introduction

Severe plastic deformation (SPD) processing significantly improves the mechanical properties of a broad range of metallic materials due to the formation of an ultrafine-grained (UFG) structure, ensuring the concurrent action of several mechanisms of strengthening thanks to the hardening contributions of solid solution, precipitations and particles, defect structures and, primarily, grain refinement [1–7]. A high-strength state is provided by controlling the microstructural parameters that are sensitive to SPD processing regimes. SPD parameters that have the greatest effect on the microstructure are strain, temperature and loading route. The latter has an effect on both the kinetics of microstructural evolution and the homogeneity of the produced microstructure. For example, when studying the microstructure transformation of Ti alloys with a change of the deformation path, it was shown that the substitution of a monotonic loading with an essentially non-monotonic one enabled activation of new slip systems and thus intensified the process of microstructural refinement [8,9]. With respect to SPD processing, it was demonstrated that the so-called route of equal-channel angular pressing (ECAP) has a great effect on structural evolution [10,11]. The best results, in terms of microstructure refinement and enhancement of mechanical properties, were obtained when using routes B and Bc, in which the billet is rotated by 90° around its axis between ECAP passes. Such a turn changes the schemes of the principal stresses and strains in a material, and as a result, the deformation process becomes non-monotonic. A similar result was obtained for the cyclic HPT when sufficient grain refinement in Ni

and Fe was reported to be achieved at a smaller deformation level than for the one-direction HPT [12]. A vivid example of non-monotonic loading is the SPD technique of multiple forging, in which the change of the scheme of principal stresses is achieved as a result of a consecutive rotation of the billet around three axes [13,14].

It is possible to realize the non-monotonic loading process through a consecutive processing of billets by different methods. This procedure has already been tested successfully for Ti-based [15], Cu-based [16] and Al-based alloys [17,18]. At the first stage of processing, SPD by ECAP-Conform was conducted, and at the second stage, rolling or drawing was performed. It is noted in all studies that a change in the type of loading had a beneficial effect on the properties of the produced materials. At the second stage of processing, an additional increase was observed in the microhardness and strength of UFG materials which had been produced by SPD at the first stage of processing. It is more difficult to unambiguously determine the effect of a change in the deformation type of producing UFG materials on the features of their microstructure. At the present time, the experimental data reported in the literature are not sufficient to summarize the results, especially for steels. Besides, of great importance is the microstructure formed immediately during SPD processing, as well as the nature of the material itself. After the rolling of even an equiaxed UFG structure, a structure was observed that was elongated in the direction of plastic straining. For copper, an increase in the structural homogeneity was revealed [16], and conversely, for an Al alloy, a separation of microstructure into two fractions was observed, one of which contained shear bands, and the other one contained equiaxed grains [17].

In this paper, we investigate the possibility of increasing the strength of an austenitic stainless steel through the use of combined strain processing. For this type of steel it is practically impossible to increase strength by thermal treatment, and thus microstructure refinement by deformation processing is an efficient means of strengthening.

2. Materials and Methods

Austenitic stainless steel was selected as an object of investigation. The chemical composition of the steel is given in Table 1. In order to produce a single-phase austenitic structure prior to SPD processing, the steel was water-quenched from a temperature of 1050 °C (exposure time 1 h). The SPD processing of rods with a diameter of 10 mm and a length of 100 mm was conducted by ECAP through 8 passes via route Bc at a temperature of 400 °C. The intersection angle of channels in the die-set was 120° (Figure 1).

Table 1. Chemical composition (wt. %) of the austenitic steel under investigation.

C	Cr	Ni	Ti	Si	S	P	Fe
0.08	16.19	9.13	0.3	0.58	0.03	0.08	bas.

The thermal conditions of ECAP processing were selected in accordance with earlier studies [6,19] that demonstrated the efficiency of SPD processing for microstructure refinement and enhancement of the mechanical properties of the austenitic stainless steel at the given temperature, as well as for the formation of grain-boundary segregations and nanotwins resulting in additional strengthening. The number of passes was selected in such a way as to be sufficiently large to impose such a strain under which the hardness and strength of a UFG billet reach saturation. The produced UFG state is further referred to as “ECAP”.

Rolling was conducted in smooth rolls at the same temperature of billet heating, 400 °C, through 15 passes to a final strip thickness of 2.3 mm. The total reduction was 77% (Figure 1). The produced UFG state is further referred to as “ECAP + Rol”. This regime was selected on the basis of the above-mentioned considerations, as well as to preserve the integrity of the billet.

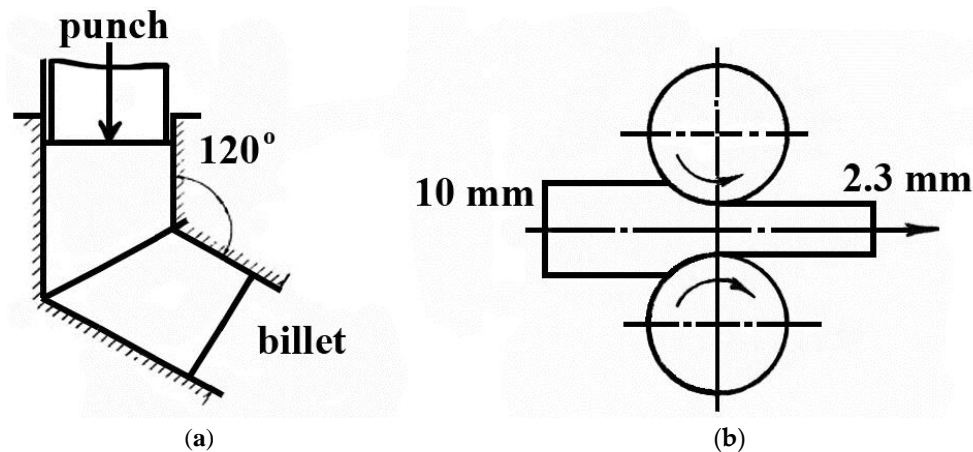


Figure 1. The principle of the combined processing of the steel (a) Stage I—ECAP, (b) Stage II—Rolling.

To study the effect of the combined processing on the microstructure and properties, we also investigated the billets subjected to rolling under the same conditions, but without a preliminary deformation processing by ECAP. This state is further referred to as “Rol”.

The microstructure was studied in the longitudinal section of a rod and a strip. To investigate the microstructure, electrolytic etching was performed in a chemically pure nitric acid (the mass fraction of the acid was at least 65%). The etching time was from 5 to 10 s under a voltage of 13–20 V. Structural studies were performed using an Olympus GX51 optical microscope (Olympus Corp, Tokyo, Japan), a JEOL JSM-6490VL scanning electron microscope (Jeol Ltd, Tokyo, Japan) and a JEOL JEM-2100 transmission electron microscope (Jeol Ltd, Tokyo, Japan). The grain sizes were determined from the dark-field images of the microstructure. At least 300 grains were measured for each condition. The dislocation density ρ_{XRD} was determined from the results of X-ray studies according to the expression [20]:

$$\rho_{\text{XRD}} = \frac{2\sqrt{3} \langle \varepsilon^2 \rangle^{1/2}}{b \cdot d_{\text{XRD}}}$$

where $\langle \varepsilon^2 \rangle^{1/2}$ is the level of elastic microdistortions of the crystal lattice; b is the Burgers vector of dislocations; d_{XRD} is the size of coherent scattering domains.

Microhardness was measured on a Micromet-5101 device in the longitudinal direction. At least 30 measurements were made for each condition. Uniaxial tensile testing was performed on an INSTRON 8801 tensile testing machine (Instron Eng. Corp., High Wycombe, UK) at room temperature. For the tensile tests, flat samples with a gauge length of 4 mm were used, the strain rate was 10^{-3} s^{-1} .

3. Results

The microstructure of the steel in the as-received state was represented by equiaxed austenite grains with a mean size of $(9 \pm 2) \mu\text{m}$ (Figure 2a). In some grains, twins were observed. The volume fraction of grains containing twins was about 10%.

After quenching, the size of austenite grains increased up to an average value of $(40 \pm 11) \mu\text{m}$. Practically all grains contained wide twins. At the boundaries of austenite grains and at twin boundary/grain boundary intersections, serrations were observed.

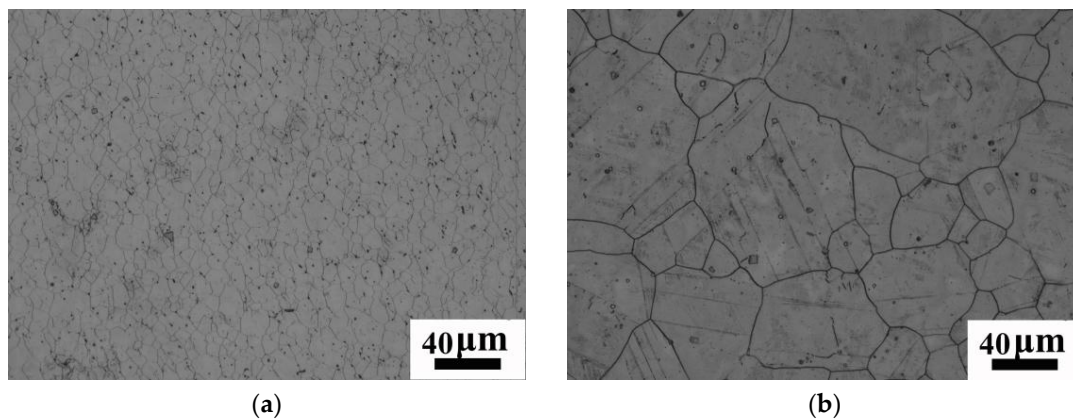


Figure 2. Microstructure of the austenitic steel: as-received condition (a); after quenching (b).

3.1. Microstructure of the Austenitic Steel after SPD Processing and Rolling

After SPD processing by ECAP, within the austenite grains we observed the formation of differently-directed shear bands (Figure 3a—the sample axis is vertical). As a result of the intersection of these bands, new boundaries form and grain refinement takes place. The microstructure is heterogeneous. At 10,000 times magnification (Figure 3b), relatively coarse grains with sizes of several μm and fine grains with sizes much smaller than 1 μm are visible. The coarse grains are elongated in the direction of the sample axis (Figure 3a). The volume fraction of the regions with relatively coarse grains amounts to about 10%.

When the structure was examined in detail by TEM, structural heterogeneity was also revealed (Figure 3c). A large volume of the structure (about 60%) is represented by shear bands with thin boundaries, within which a developed dislocation structure in the form of wide dislocation boundaries is observed. These boundaries divide the bands into non-equiaxed cells. The cell size amounts to, on average, about 180 nm in the transverse direction and 370 nm in the longitudinal direction (Figure 3c). Alongside shear bands, practically equiaxed grains with a reduced dislocation density and thin equilibrium boundaries are present in the structure. The grain size is about 350 nm. Separate deformation twins are observed in the grains (about 10 nm in thickness) (Figure 3d). The fraction of grains with twins does not exceed 5%. The average spacing between the twin boundaries is about 75 nm. The selected area electron diffraction pattern shown in the insert in Figure 3c reveals separate reflections located circumferentially, which indicates high-angle misorientations of grain boundaries.

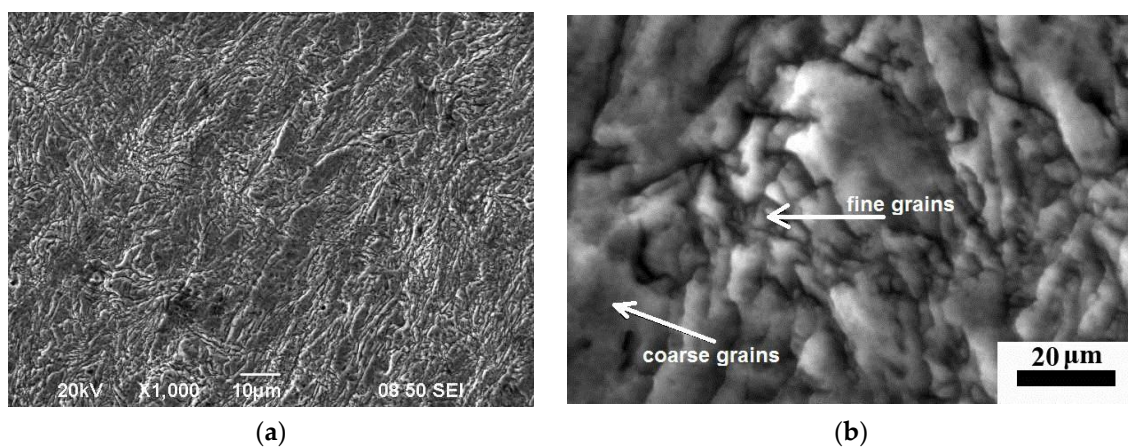


Figure 3. Cont.

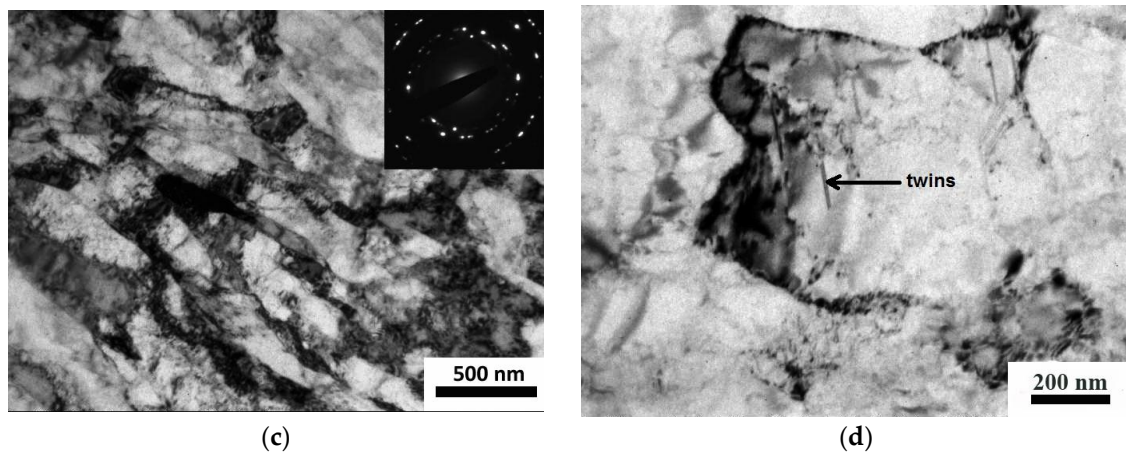


Figure 3. Microstructure of the steel after SPD processing (via ECAP) in the longitudinal section (“ECAP” condition): (a,b) SEM; (c,d) TEM, the aperture size for diffraction patterns $\sim 1 \mu\text{m}^2$.

Thus, after SPD processing via ECAP, a heterogeneous austenitic UFG structure is formed. This structure consisted of grains/subgrains elongated in the direction of straining, with a small number of twins.

After rolling of the ECAP-processed steel, further grain refinement is observed (Figure 4). Individual grains are practically not identified by an optical microscope. The boundaries of the original austenite grains are not visible either (Figure 4a).

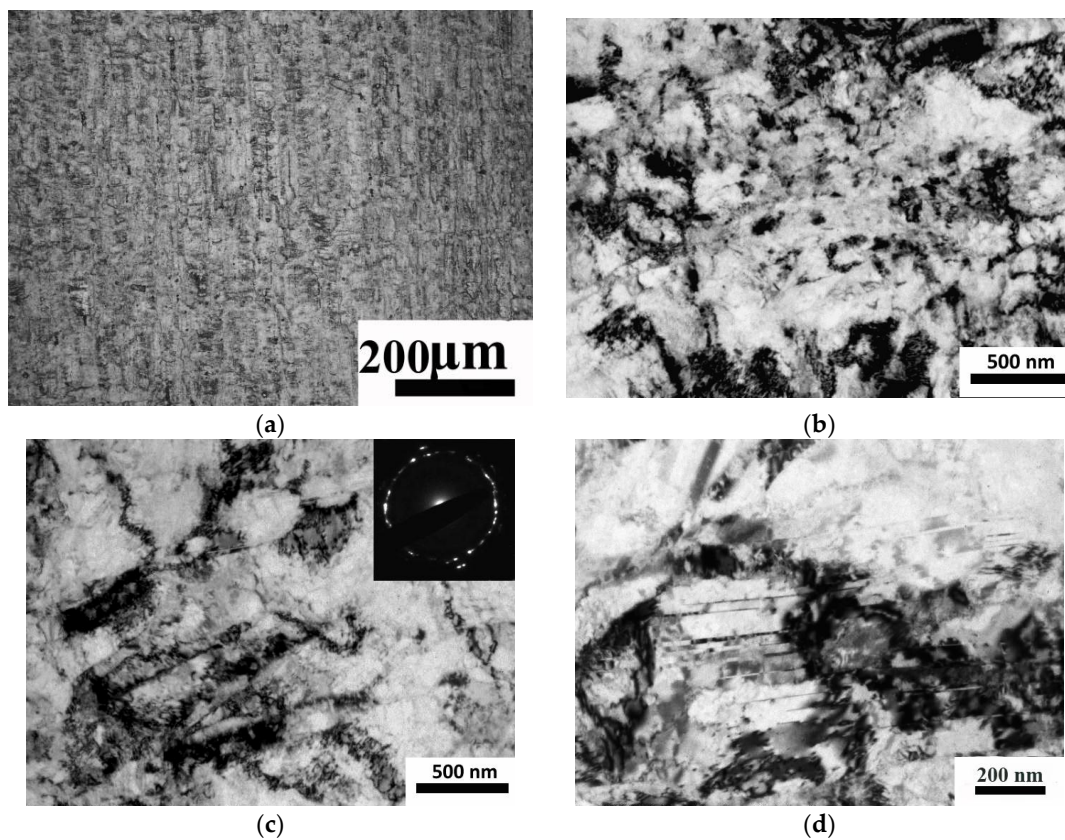


Figure 4. Structure of the austenitic steel after ECAP and subsequent rolling to a total reduction in area of 77% (“ECAP + Rol” condition): (a) optical microscopy; (b–d) TEM, the aperture size for diffraction patterns $\sim 1 \mu\text{m}^2$.

When the microstructure is examined by TEM, it can be seen that the microstructure has become more homogeneous (Figure 4b) as compared to the one observed in the “ECAP” state (Figure 3c). The structure has a grain/cellular character. Shear bands are preserved in separate regions, but the fraction of banded structure is only about 10%. The dislocation density increases, while the size of structural elements decreases to 110 nm. Thin twins are observed in the grains (Figure 4d). The fraction of grains containing twins increases to 14%. The average twin spacing decreases to 30 nm. The electron diffraction pattern shown in the insert of Figure 4c has a ring-shaped form, which indicates high-angle misorientation between grains. Thus, combined loading leads to further microstructure refinement—the mean grain size decreases to 110 nm, and the fraction of nanotwins grows.

In the steel samples after rolling (“Rol” condition) the boundaries of original austenite grains (Figure 5a), elongated in the rolling direction are still observed. Formation of shear bands is distinctly observed within the grains there. At the boundaries of the original austenite grains and at the shear band/grain boundary intersections, ledges are seen. A banded structure (Figure 5b,c) is also observed in some areas. Inside the bands there are wide boundaries dividing grains into cells (Figure 4b–d). The average cell size amounts to 560 nm. The structure is characterized by an increased dislocation density. Twins are almost absent. Thus, in the “Rol” condition, the steel is characterized by a banded cellular structure with a cell size of 560 nm, which does not contain twins.

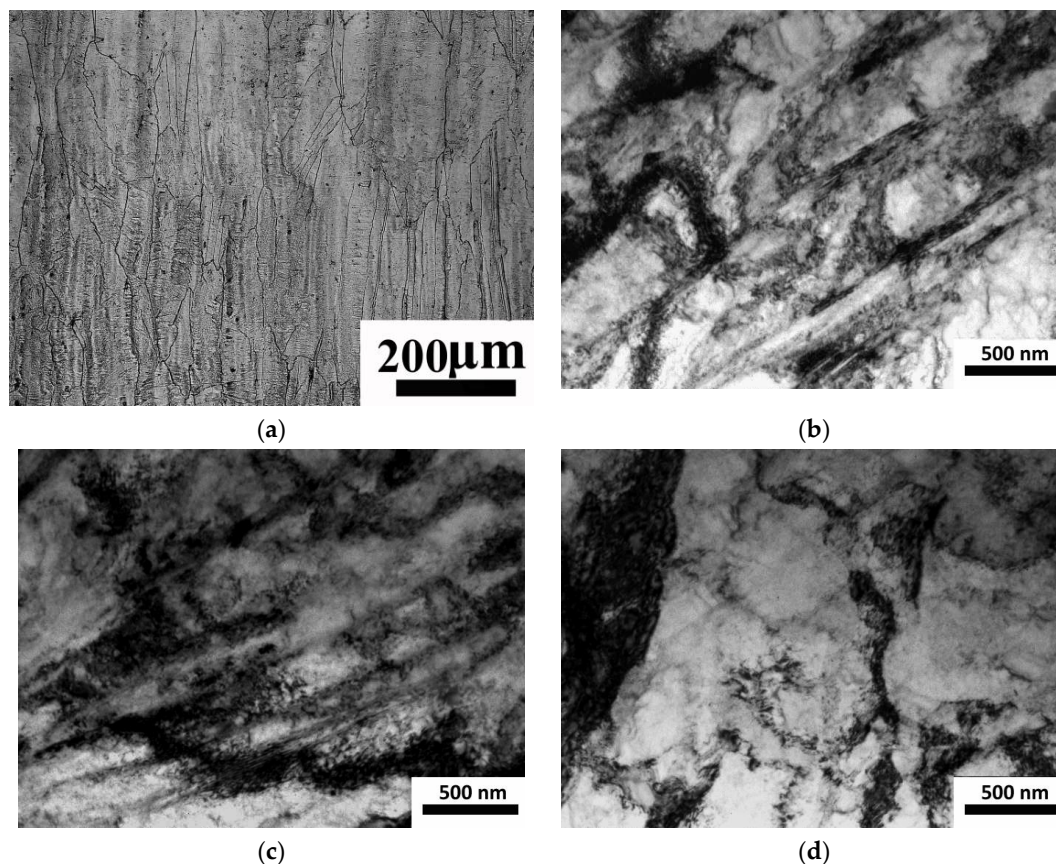


Figure 5. Microstructure of the austenitic steel after rolling to a total reduction in area of 77% (“Rol” condition): (a) optical microscopy; (b–d) TEM.

3.2. Mechanical Properties of the Austenitic Steel

The average microhardness value of the austenitic steel in the as-received state consists (1970 ± 60) MPa (Figure 6). After quenching microhardness declines slightly to a value of (1820 ± 30) MPa, which is related to the growth of austenite grains, as well as to a more complete dissolution of excess phases during heating prior to quenching.

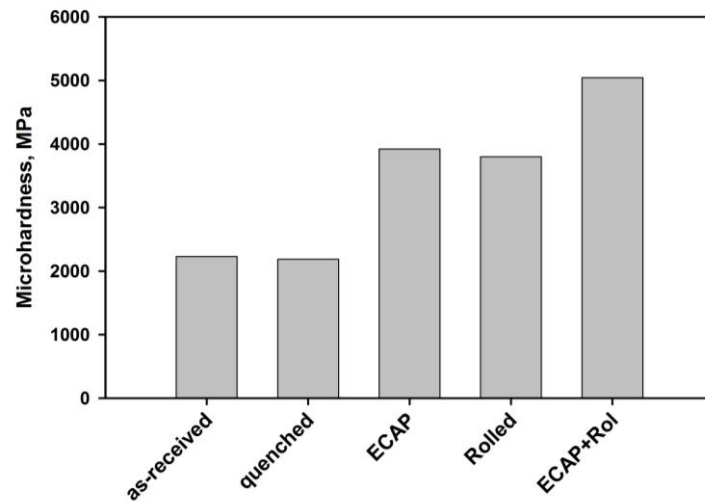


Figure 6. Microhardness of the austenitic steel after different types of processing.

As a result of microstructure refinement, in the “ECAP” state the average microhardness value of the steel grows two-fold, reaching (3920 ± 50) MPa. After rolling to 77% without a preliminary ECAP processing (“Rol”), there is also observed an increase in hardness, very similar to ECAP processing—to 3800 ± 50 MPa. A combination of ECAP and rolling results in an even greater increase in microhardness, namely 33%, reaching (5040 ± 40) MPa (Figure 6).

In a similar manner, straining has an effect on the steel’s strength as well. Figure 7 shows the engineering stress-strain curves obtained during tensile tests of the steel samples in different state. It is obvious that the deformation behavior of the material changes depending of the type of processing of the steel. The quantitative data on the mechanical properties of the steel in different state are summarized in Table 2. Peculiar to the quenched condition there is a significant capability for strengthening: the yield stress is $\sigma_{0.2} = 200$ MPa, the ultimate tensile strength (UTS) is 2.5 times higher— $\sigma_{\text{ult}} = 720$ MPa. The elongation is $\delta = 65\%$.

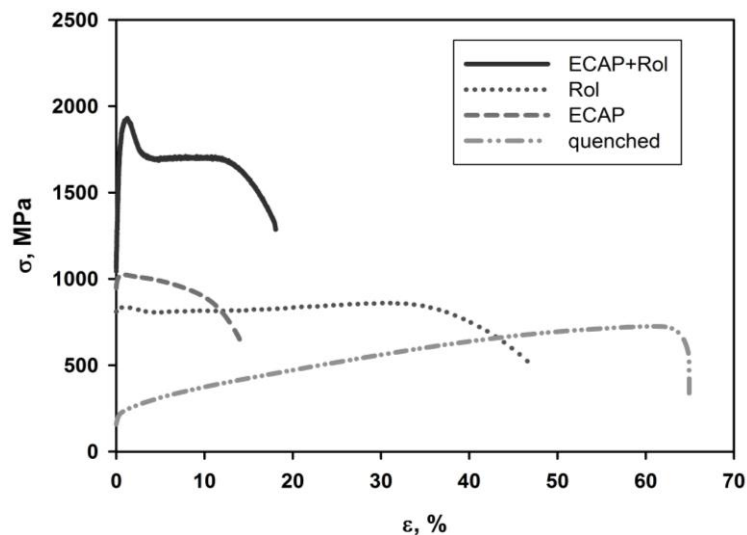


Figure 7. Engineering stress-strain curves of the steel after different types of processing.

Table 2. Mechanical properties of the steel after different types of processing.

Condition	Offset Yield Stress $\sigma_{0.2}$ (MPa)	Upper Yield Stress (Corresponds to Yield Drop) σ_{BU} (MPa)	Lower Yield Stress (Corresponds to Yield Plateau) σ_1 (MPa)	Ultimate Tensile Strength σ_{ult} (MPa)	Uniform Elongation $\delta_{uniform}$ (%)	Elongation to Failure δ (%)	Microhardness (MPa)
quenching	200	-	-	720	62	65	1820
ECAP	950	-	-	1020	1	14	3920
Rol	-	830	800	855	33	47	3800
ECAP + Rol	-	1925	1700	1720	11	18	5040

The steel in the “ECAP” state is characterized by a high value of yield stress $\sigma_{0.2} = 950$ MPa with a very short period of insignificant strengthening: the uniform elongation is only 1%, the UTS is $\sigma_{\text{ult}} = 1020$ MPa. After that, a rapid strain localization and necking take place, corresponding to the region with a stress decline in the diagram. The total elongation is $\delta = 14\%$. In spite of similar values of microhardness and yield stress in the “ECAP” and “Rol” states, the deformation behavior of those differs significantly. In the curve of the rolled sample, there appears a weakly expressed yield drop, corresponding to the upper yield stress $\sigma_u = 830$ MPa. After that there is observed a yield plateau, corresponding to the lower (physical) yield stress $\sigma_l = 800$ MPa and the region of weak strengthening. The UTS is $\sigma_{\text{ult}} = 855$ MPa, the elongation to failure is $\delta = 47\%$. The highest strength is exhibited by the samples after the “ECAP + Rol” combined loading. This state is displayed by the curve with a distinct yield drop. The upper yield stress is $\sigma_u = 1925$ MPa, and the lower yield stress, corresponding to the yield plateau, is $\sigma_l = 1700$ MPa. The curve does not demonstrate notable strengthening, strain localization starts as the elongation reaches the value $\delta = 11\%$, and the total elongation is $\delta = 18\%$.

Thus, the type of deformation processing determines not only the level of properties, but also the tensile mechanical behavior of the steel.

4. Discussion

Numerous studies on the SPD processing of bulk metallic billets via ECAP have demonstrated that the increase in hardness and strength is observed after the initial one or two passes, after which further strengthening becomes much slower [21–23]. Meanwhile, the possibilities for strength enhancement in a material have not yet been exhausted. This is confirmed by the fact that under processing by high-pressure torsion, as a rule, the observed hardness values are significantly larger than the ones that can be attained by ECAP processing [10].

Microstructural features of metallic materials provide activation of the related deformation mechanisms, which, in their turn, contribute to the strengthening of the given material. Varying SPD parameters one can purposefully form the targeted features in the produced UFG materials and put into action the corresponding strengthening mechanisms. In UFG materials produced by SPD, strengthening can be achieved due to several mechanisms [1–7,23]:

1. Grain-boundary and dislocation strengthening. During the grain refinement the volume fraction of grain boundaries, which are an efficient impediment for dislocation movement, significantly increases. For the formation of new strain-induced boundaries, dislocation generation in various slip systems is necessary.

When analyzing the types of loading realized in the course of SPD, it is necessary to mention two distinctive features typical of SPD processing:

- a. a high hydrostatic constituent, which is especially significant in high-pressure torsion, but present in all deformation techniques;
- b. an essential non-monotony of strain, typical for most SPD techniques, such as ECAP or multiple forging.

Both of these features enable activating additional slip systems, thus leading to an increase in dislocation density, formation of new interfaces and microstructure refinement.

2. Solid-solution strengthening and precipitation hardening. These mechanisms are competing ones, since as a result the alloying of a solid solution, the corresponding strengthening grows, but the amount of dispersed particles (providing precipitation hardening) decreases. The contribution of these constituents to strengthening is determined primarily by the deformation temperature. It has been shown [24,25] that at room temperature the dissolution of second-phase particles prevails, but as the deformation temperature is increased, precipitation is observed.

3. Formation of segregations at grain boundaries. This process is also connected with the solid solution decomposition during SPD and a transfer of solute atoms to the boundaries. The action of this mechanism is also thermally dependent: at room temperature no segregations were observed, and at elevated temperatures the formation of the grain boundary segregations was shown [5,26].
4. Formation of twins. For a number of materials, including austenitic steels, it is typical that nanotwins form during SPD processing. The high-angle boundaries of nanotwins are also impediments for dislocation movement and, consequently, they provide additional strengthening. Twinning may be activated when possibilities for slip are limited. When the scheme of the stress-strain state is changed (in this particular case, by changing the type of loading), the direction of action of the maximum tangential stresses changes with respect to the sample's axis. As a result of such a change, new slip systems should be activated, and the activation of twinning is also possible.

Thus, a change in the loading scheme may activate at least several of the above-mentioned factors of strengthening: an increase in dislocation density, grain refinement and an increase in the fraction of twins. These conclusions are confirmed by studies conducted on various materials. For instance, in [17], in the Al alloy 5083 after ECAP processing and additional compression, imitating rolling conditions, an increase in dislocation density was observed. An enhancement of strength after ECAP-Conform processing and compression of Ti [15], after ECAP processing and rolling of Cu [16], was accounted for by the formation of additional low-angle boundaries within grains and a transformation of the low-angle boundaries into high-angle ones. This conclusion is also consistent with the studies on the microstructure of austenitic steel in different states reported in the present study (see Table 3).

Table 3. Features of the structure of steel after straining.

Condition	Dislocation Density (m^{-2})	Grain/Cell Size (nm)	Fraction of Shear Bands	Fraction of Grains with Twins (%)	Twin Spacing (nm)
ECAP	1.28×10^{14}	350	60	5	75
ECAP + Rol	7.19×10^{14}	110	10	14	30
Rol	4.27×10^{14}	560	80	-	-

Comparison of the microstructural parameters of steel in different states demonstrates that the size of structural elements considerably decreases as compared with the “ECAP” and the “Rol” states as a result of combined loading. This leads to a considerable increase in the density of grain boundaries.

Let us consider a generalized dependence of yield stress on grain size in terms of the Hall-Petch relation, presented on the basis of literature data in Figure 8.

The results obtained in the present study are also presented in the graph. It can be seen that the points corresponding to the “ECAP” or “Rol” states have a certain deviation from the line summarizing literature data towards larger values of yield stress. Moreover, the point corresponding to the “ECAP + Rol” condition is located much higher than expected in accordance with the Hall-Petch relation.

As considered above, strengthening of nanostructured steels is provided not only by grain size. For austenitic steels, additional strengthening is introduced by the dislocation mechanism, as well as by twin boundaries, as was demonstrated in [6]. In the general case, the contributions of different mechanisms follow linear additivity [2,3,5–7,23]:

$$\Delta\sigma_y = \Delta\sigma_{FS} + \Delta\sigma_{SS} + \Delta\sigma_\ell + \Delta\sigma_{GB}$$

where σ_{FS} is the friction stress of γ -iron's lattice; $\Delta\sigma_{SS}$ is solid-solution strengthening; $\Delta\sigma_\ell$ is dislocation strengthening; $\Delta\sigma_{GB}$ is grain-boundary strengthening.

Let us estimate the contribution of these mechanisms into the yield stress of the investigated steel in each state.

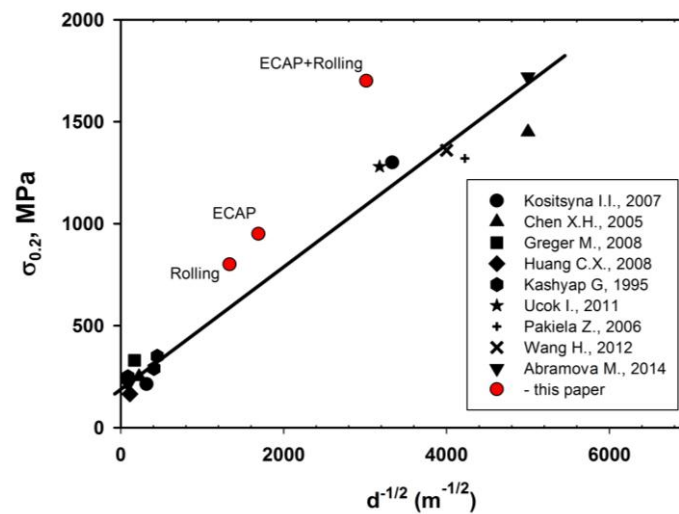


Figure 8. Hall-Petch relation for chromium-nickel austenitic steels, built on the basis of literature data [6,27–34] (back marks) and the results of the present study (red marks).

The lattice friction stress and solid solution hardening can be defined from the Hall-Petch relation, displayed in Figure 8, as the stress corresponding to the infinitely large grain size. In the given case, it is $\Delta\sigma_0 = 195$ MPa.

Dislocation strengthening can be estimated according to:

$$\Delta\sigma_d = \alpha MbG\varrho^{1/2}$$

where $\alpha = 0.3$ is a constant; $M = 3.05$ is the Taylor factor; $G = 77$ GPa is the shear modulus and $b = \sqrt{2}a/2$ is the Burgers vector for the investigated steel.

Let us define additional grain-boundary strengthening, taking into account the presence of twins, as [6]:

$$\Delta\sigma_{GB} = (1 - f)k_y d^{-1/2} + f k_y \lambda^{-1/2}$$

where f is the fraction of grains with twins; $k_y = 0.3$ MPa·m^{1/2} is a constant derived from the dependence in Figure 8; d is the average grain/cell size; λ is the average twin spacing.

The results of the analysis are given in Table 4.

Table 4. Calculated results for the contribution of different mechanisms to the strengthening of the steel.

Condition	$\Delta\sigma_0$	$\Delta\sigma_{GB}$			Calculated Value	Experimental Value
		$\Delta\sigma_d$	$\Delta\sigma_{tw}$	$\Delta\sigma_d + \Delta\sigma_{tw}$		
ECAP	202	481	55	536	933	950
ECAP + Rol	480	778	242	1020	1688	1700
Rol	370	401	-	401	771	800

The calculated yield stress values are very close to the experimental ones. Microstructural studies and the presented estimations show that strength enhancement of the steel under a combined loading is provided predominantly by the grain-boundary hardening contribution in accordance with the Hall-Petch equation. Besides, unlike in ECAP processing, no twins were observed in the structure of the steel after rolling at a temperature of 400 °C. After the combined loading, the fraction of twins

increases even compared to the “ECAP” state, and this component also notably contributes to the steel’s strengthening (see Table 4). The dislocation contribution into yield stress grows almost two-fold.

In addition to further strengthening, the combined “ECAP + Rol” loading also has an effect on the steel’s deformation behavior, which is principally different not only from the quenched state, but also from the steel’s behavior in the “ECAP” and “Rol” states. In the quenched state, the microstructure is characterized by a small density of grain boundaries and wide twins. After straining dislocation density increases, and as a result, an extensive region of strengthening and a high value of ductility are observed in the curve. In the “ECAP” state the stress-strain curve is typical for materials subjected to SPD—the maximum stress is achieved at early deformation stage, then rapid localization of strain and failure occur.

After “ECAP + Rol” treatment, a distinct yield drop is observed in the curve. Its appearance could be caused by segregations. The formation of segregations during elevated temperature SPD processing was found in recent years in SPD alloys, including austenitic steels [6]. In the samples after rolling, the appearance of a weakly expressed yield drop could indicate the formation of segregations or atmospheres pinning dislocations. Evidently, the formation of a UFG structure with a high density of grain boundaries during ECAP processing stimulates segregation formation during subsequent rolling, which is expressed in the yield phenomenon observed in the curve. The contribution of segregations can be estimated as the difference between the upper and the lower yield stresses, which amounts to 225 MPa for the steel in the “ECAP + Rol” condition. However, this issue requires an additional detailed study.

It should be noted that the steel after “ECAP + Rol” is characterized by rather high values of both uniform (11%) and total (18%) elongation. This may also be related to the pinning of dislocations by atmospheres or segregations of solutes: after the disruption of the blocking of a large quantity of dislocations, their free movement is possible, thus ensuring an additional deformation of the sample.

Thus, the application of the combined “ECAP + Rol” technique results in a considerable growth in the density of grain boundaries and increases the dislocation density and fraction of twins in the microstructure, which enables enhancement of the strength characteristics, while at the same time preserving the ductility of the UFG austenitic steel.

5. Conclusions

- (1) A combination of SPD processing and a conventional metal forming technique for the rolling of austenitic steel leads to a further refinement of a homogeneous UFG cell-granular microstructure with a high density of grain boundaries and a large fraction of twins.
- (2) As a result, the tensile mechanical behavior of the UFG steel samples produced by the combined “ECAP + Rol” loading changes—it exhibits a yield drop, to which corresponds the upper yield stress of 1925 MPa, as well as a yield plateau, and the yield stress amounts to 1700 MPa. The obtained values of strength are 1.5 times higher than the values of yield stress obtained when using only the ECAP technique (950 MPa) or only rolling (~815 MPa). Besides, in the UFG sheet produced by combined loading, a rather reasonable level of ductility is preserved: a uniform elongation of 11% and a total elongation of 18%.
- (3) The enhancement of the strength characteristics is achieved as a result of a combined action of several strengthening mechanisms: grain-boundary strengthening, dislocation strengthening, twinning-induced strengthening and, presumably, strengthening due to the formation of solute segregations in grain boundaries.

Acknowledgments: The authors acknowledge the financial support from the Ministry of Education and Science of the Russian Federation under Grant Agreement No. 14.583.21.0012 (unique identification number RFMEFI58315X0012) and by the International Research & Development Program of the National Research Foundation of Korea (NRF) funded by the Ministry of Science, ICT and Future Planning (MSIP) of Korea (Grant No. K1A3A1A49.070466, FY2014). A part of investigations was conducted using the facilities of the

Common Use Center Nanotech (Ufa State Aviation Technical University) and Centre for X-ray Diffraction Studies (Research Park of Saint-Petersburg State University).

Author Contributions: M.V.K. fulfilled the general analysis of results, estimation of hardening contributions and she was responsible for writing the manuscript; M.M.A. was dealing with processing by rolling, specimen preparation, TEM measurements and mechanical testing of the samples; N.A.E. was responsible for XRD analysis and data processing as well as for discussion of hardening mechanisms; G.I.R. conducted ECAP-processing; R.Z.V. participated in task definition and performed general supervision of the conducted studies All authors contributed to discussion and summarizing of results as well as to correction and revisions of the manuscript.

Conflicts of Interest: The authors declare no conflict of interest.

References

1. Valiev, R.Z.; Horita, Z.; Langdon, T.G.; Zehetbauer, M.J.; Zhu, Y.T. Fundamentals of superior properties in bulk nano SPD materials. *Mater. Res. Lett.* **2016**, *4*, 1–21. [[CrossRef](#)]
2. Valiev, R.Z.; Enikeev, N.A.; Langdon, T.G. Towards superstrength of nanostructured metals and alloys, produced by SPD. *Met. Mater.* **2011**, *49*, 1–9.
3. Hasan, H.S.; Peet, M.J.; Avettand-Fénoël, M.-N.; Bhadeshia, H.K.D.H. Effect of tempering upon the tensile properties of a nanostructured bainitic steel. *Mater. Sci. Eng. A* **2014**, *615*, 340–347. [[CrossRef](#)]
4. Valiev, R.Z.; Estrin, Y.; Horita, Z.; Langdon, T.G.; Zehetbauer, M.J.; Zhu, Y.T. Producing Bulk Ultrafine-Grained Materials by Severe Plastic Deformation: Ten Years Later. *JOM* **2016**, *68*, 1216–1226. [[CrossRef](#)]
5. Kamikawa, N.; Abe, Y.; Miyamoto, G.; Funakawa, Y.; Furuhashi, T. Tensile behavior of Ti, Mo-added low carbon steels with interphase precipitation. *ISIJ Int.* **2014**, *54*, 212–221. [[CrossRef](#)]
6. Abramova, M.M.; Enikeev, N.A.; Valiev, R.Z.; Etienne, A.; Radiguet, B.; Ivanisenko, Y.; Sauvage, X. Grain boundary segregation induced strengthening of an ultrafine-grained austenitic stainless steel. *Mater. Lett.* **2014**, *136*, 349–352. [[CrossRef](#)]
7. Ganeev, A.V.; Karavaeva, M.V.; Sauvage, X.; Courtois-Manara, E.; Ivanisenko, Y.; Valiev, R.Z. On the nature of high-strength of carbon steel produced by severe plastic deformation. *IOP Conf. Ser. Mater. Sci. Eng.* **2014**, *63*. [[CrossRef](#)]
8. Bylja, O.I.; Vasin, R.A.; Ermachenko, A.G.; Karavaeva, M.V.; Muravlev, A.V.; Chistjakov, P.V. The influence of simple and complex loading on structure changes in two-phase titanium alloy. *Scr. Mater.* **1997**, *36*, 949–954. [[CrossRef](#)]
9. Berdin, V.K.; Karavaeva, M.V.; Syutina, L.A. Effect of the type of loading on the evolution of microstructure and crystallographic texture in VT9 titanium alloy. *Met. Sci. Heat Treat.* **2003**, *45*, 423–427. [[CrossRef](#)]
10. Valiev, R.Z.; Zhilyaev, A.P.; Langdon, T.G. *Bulk Nanostructured Materials: Fundamentals and Applications*; John Wiley & Sons, Inc.: New York, NY, USA, 2014; p. 456.
11. Iwahashi, Y.; Horita, Z.; Nemoto, M.; Langdon, T.G. The process of grain refinement in equal-channel angular pressing. *Acta Mater.* **1998**, *46*, 3317–3331. [[CrossRef](#)]
12. Wetscher, F.; Pippan, R. Cyclic high-pressure torsion of nickel and ARMCO iron. *Philos. Mag.* **2006**, *86*, 5867–5883. [[CrossRef](#)]
13. Salishev, G.; Zaripova, R.; Galeev, R.; Valiahmetov, O. Nanocrystalline structure formation during severe plastic deformation in metals and their deformation behavior. *Nanostruct. Mater.* **1995**, *6*, 913–916. [[CrossRef](#)]
14. Belyakov, A.; Tsuzaki, K.; Kaibyshev, R. Nanostructure evolution in an austenitic stainless steel subjected to multiple forging at ambient temperature. *Mater. Sci. Forum* **2011**, *667–669*, 553–558. [[CrossRef](#)]
15. Polyakov, A.; Gunderov, D.; Sildikov, V.; Valiev, R.; Semenova, I.; Sabirov, I. Physical simulation of hot rolling of ultra-fine grained pure titanium. *Metall. Trans. B* **2014**, *45B*, 2315–2326. [[CrossRef](#)]
16. Stepanov, N.D.; Kuznetsov, A.V.; Salishev, G.A.; Raab, G.I.; Valiev, R.Z. Effect of cold rolling on microstructure and mechanical properties of copper subjected to ECAP with various number of passes. *Mater. Sci. Eng. A* **2012**, *554*, 105–115. [[CrossRef](#)]
17. Murashkin, M.Y.; Enikeev, N.A.; Kazykhanov, V.U.; Sabirov, I.; Valiev, R.Z. Physical simulation of cold rolling of ultra-fine grained Al 5083 alloy to study microstructure evolution. *Rev. Adv. Mater. Sci.* **2013**, *35*, 75–85.
18. Sabbaghianrad, S.; Langdon, T.G. Microstructural saturation, hardness stability and superplasticity in ultrafine-grained metals processed by a combination of severe plastic deformation techniques. *Lett. Mater.* **2015**, *5*, 335–340. [[CrossRef](#)]

19. Vorhauer, A.; Kleber, S.; Pippan, R. Influence of processing temperature on microstructure and mechanical properties of high-alloyed single-phase steels subjected to severe plastic deformation. *Mater. Sci. Eng. A* **2005**, *410–411*, 281–284. [[CrossRef](#)]
20. Williamson, G.K.; Smallman, R.E. III. Dislocation densities in some annealed and cold-worked metals from measurements on the X-ray Debye-Scherrer spectrum. *Philos. Mag.* **1956**, *1*, 34–45. [[CrossRef](#)]
21. Dobatkin, S.V.; Rybal'chenko, O.V.; Raab, G.I. Structure formation, phase transformations and properties in Cr-Ni austenitic steel after equal-channel angular pressing and heating. *Mater. Sci. Eng. A* **2007**, *463*, 41–45. [[CrossRef](#)]
22. Pang, J.C.; Yang, M.X.; Yang, G.; Wu, S.D.; Li, S.X.; Zhang, Z.F. Tensile and fatigue properties of ultrafine-grained low-carbon steel processed by equal channel angular pressing. *Mater. Sci. Eng. A* **2012**, *553*, 157–163. [[CrossRef](#)]
23. Whang, S.H. *Nanostructured Metals and Alloys. Processing, Microstructure, Mechanical Properties and Applications*; Woodhead Publishing Limited: Cambridge, UK, 2011.
24. Ivanisenko, Y.; Lojkwski, W.; Valiev, R.Z.; Fecht, H.-J. The mechanism of formation of nanostructure and dissolution of cementite in a pearlitic steel during high pressure torsion. *Acta Mater.* **2003**, *51*, 5555–5570. [[CrossRef](#)]
25. Karavaeva, M.V.; Nurieva, S.K.; Zaripov, N.G.; Ganeev, A.V.; Valiev, R.Z. Microstructure and mechanical properties of medium-carbon steel subjected to severe plastic deformation. *Met. Sci. Heat Treat.* **2012**, *4*, 1–5. [[CrossRef](#)]
26. Ganeev, A.V.; Karavaeva, M.V.; Sauvage, X.; Ivanisenko, Y.; Valiev, R.Z. The grain-boundary precipitates in ultrafine-grained carbon steels produced by HPT. In Proceedings of the XV International Conference on Intergranular and Interphase Boundaries in Materials, Moscow, Russia, 23–27 May 2016.
27. Kositsyna, I.I.; Sagaradze, V.V. Phase transformations and mechanical properties of stainless steel in the nanostructural state. *Bull. Russ. Acad. Sci. Phys.* **2007**, *71*, 293–296. [[CrossRef](#)]
28. Chen, X.H.; Lu, J.; Lu, L.; Lu, K. Tensile properties of a nanocrystalline 316L austenitic stainless steel. *Scr. Mater.* **2005**, *52*, 1039–1044. [[CrossRef](#)]
29. Greger, M.; Vodárek, V.; Dobrzański, L.A.; Kander, L.; Kocich, R.; Kufetová, B. The structure of austenitic steel AISI 316 after ECAP and low-cycle fatigue. *J. Ach. Mater. Manuf. Eng.* **2008**, *28*, 151–158.
30. Huang, C.X.; Yang, G.; Gao, Y.L.; Wu, S.D.; Zhang, Z.F. Influence of processing temperature on the microstructures and tensile properties of 304L stainless steel by ECAP. *Mater. Sci. Eng. A* **2008**, *485*, 643–650. [[CrossRef](#)]
31. Kashyap, B.; Tangri, K. On the Hall-Petch relationship and substructural evolution in type 316L stainless steel. *Acta Mater.* **1995**, *43*, 3971–3981. [[CrossRef](#)]
32. Üçok, İ.; Ando, T.; Grant, N. Property enhancement in type 316L stainless steel by spray forming. *Mater. Sci. Eng. A* **1991**, *133*, 284–287. [[CrossRef](#)]
33. Pakieła, Z.; Garbacz, H.; Lewandowska, A.; Suś-Ryszkowska, M.; Zieliński, W.; Kurzydłowski, K. Structure and properties of nanomaterials produced by severe plastic deformation. *Nukleonika* **2006**, *51*, 19–25.
34. Wang, H.; Shuro, I.; Umemoto, M.; Kuo, H.-H.; Todaka, Y. Annealing behavior of nano-crystalline austenitic SUS316L produced by HPT. *Mater. Sci. Eng. A* **2012**, *556*, 906–910. [[CrossRef](#)]

